Available online at www.sciencedirect.com
ScienceDirect
Polymer 47 (2006) 7774–7785
polymer
www.elsevier.com/locate/polymer

Free volume in poly(*n*-alkyl methacrylate)s from positron lifetime and PVT experiments and its relation to the structural relaxation

D. Kilburn [a,b,*], G. Dlubek [a,c], J. Pionteck [d], M.A. Alam [a]

[a] *University of Bristol, H. H. Wills Physics Laboratory, Tyndall Avenue, Bristol BS8 1 TL, UK*
[b] *Indiana University Cyclotron Facility, 2401 Milo B. Sampson Lane, Bloomington, IN, USA*
[c] *ITA Institut fuer Innovative Technologien GmbH, Koethen, Aussenstelle Halle, Wiesenring 4, D-06120 Lieskau (bei Halle/S), Germany*
[d] *Leibniz-Institut fuer Polymerforschung Dresden e.V., Hohe Strasse 6, D-01069 Dresden, Germany*

Received 23 May 2006; received in revised form 21 August 2006; accepted 22 August 2006
Available online 20 September 2006

Abstract

Free volume data from positron annihilation lifetime spectroscopy (PALS) experiments are combined with a Simha–Somcynsky (S–S) equation of state analysis of pressure–volume–temperature (PVT) data to model free volume contributions to structural mobility in a series of poly(*n*-alkyl methacrylate)s. From the PALS data the glass transition temperature, T_g, decreases (from 382 to 224 ± 5 K) and a given mean free volume is observed at lower temperatures as the side-chain length increases (going from methyl- to hexyl-). This is evidence of an internal plasticization whereby the side-chains reduce effective packing of molecules. By comparing PALS and PVT data, the hole number per mass unit, N'_h, is calculated using different methods; this varies between 0.54 and 0.86×10^{21} g^{-1}. It is found that the extrapolated free volume becomes zero at a temperature T'_0 that is smaller than the Vogel temperature T_0 of the α-relaxation. The α-relaxation frequencies can be fitted by the free volume theory of Cohen and Turnbull, but only when the free volume V_f is replaced by $(V_f - \Delta V)$ where $\Delta V (= E_f(T_0 - T'_0)$, E_f is the thermal expansivity of V_f) varies between 0.060 and 0.027 ± 0.003 cm^3/g, decreasing with side-chain length, apart from poly(*n*-hexyl methacrylate) where ΔV increases to 0.043 ± 0.003 cm^3/g. One possible interpretation of this is that the α-relaxation only occurs when, due to statistical reasons, a group of *m* or more unoccupied S–S cells are located adjacent to one another. *m* is found to vary between 8 and 2 for poly(methyl methacrylate) and poly(*n*-butyl methacrylate), respectively. We found that no specific feature in the free volume expansion was consistently in coincidence with the dynamic crossover.

Keywords: Free volume; Positron; Poly(*n*-alkyl methacrylate)s

1. Introduction

The discussion about the influence of free volume on the mobility of molecules in amorphous solids has a long history in polymer science. This is because it is based on the intuitively appealing picture of molecules' motion being influenced by the space around them. This connection was empirically quantified by Doolittle [1], and has been further explored by, for example, Cohen and Turnbull (theory based on some basic assumptions and statistical mechanics) [2].

The major difficulty in fully assessing any theoretical predictions connecting free volume and molecular mobility is in measuring the free volume present. The angstrom-sized free space that exists between molecules in a material has the form of a number of interconnected 'holes' of varying sizes and shapes. A complete topographic representation of these holes is not realistic, and so an average dimension must be sought. This is achieved in the present work, as has become relatively common over the past few decades, by using positron annihilation lifetime spectroscopy (PALS) [3–5]. This technique involves the measurement of the lifetimes of

* Corresponding author. Indiana University Cyclotron Facility, 2401 Milo B. Sampson Lane, Bloomington, IN, USA. Tel.: +1 812 855 1435; fax: +1 812 855 6645.
E-mail address: dunkilbu@indiana.edu (D. Kilburn).

0032-3861/$ - see front matter © 2006 Elsevier Ltd. All rights reserved.
doi:10.1016/j.polymer.2006.08.055

positrons injected into a sample, extracting the mean lifetimes of those positrons forming *ortho*-positronium (*o*-Ps), and relating this, via a simple semi-empirical equation, to the free volume hole dimensions. The semi-empirical equation referred to, the Tao–Eldrup equation, which will be described fully later in this paper, assumes a spherical hole symmetry. This is an over-simplification, and so the resultant ramifications on interpretation have been considered. As described by Hofmann et al. [6], irregularly shaped holes can be sampled in such a way that the shortest dimension(s) of the hole is the controlling parameter in the positron's lifetime, for example: long, thin (cylindrical) holes. Holes with complex shapes, furthermore, will be sampled by test particles (*o*-Ps) in such a way as to be measured as identical to smaller, less complex, holes. Despite this relatively crude measurement of average hole size or hole size distribution, PALS remains a unique method for directly measuring the free volume holes in the bulk of a polymer.

In the era of PALS experiments therefore the opportunity has arisen for testing some theoretical approaches to molecular mobility. For example, some of the authors [7] have shown that the ionic conductivity of ethylene oxide based polymer electrolytes is determined by the local free volume as measured by PALS, via the Cohen–Turnbull model [2] and the Vogel–Fulcher–Tammann (VFT) Law [8–10], over several orders of magnitude. While the mobility of small molecules in polymers always seems to follow the free volume theory, the situation for rheological behaviour appears more complicated. Bartoš et al. [11] combined the Williams–Landel–Ferry (WLF) equation [12] with Doolittle's equation [1]. This work showed that the rheological behaviour of polyisobutylene over a wide temperature range could be shown to be governed by the free volume as detected by PALS while in the case of *cis*-1,4-polybutadiene the free volume equation must be modified by including an energy term. Results similar to the latter were also obtained by some of the authors for poly(vinyl acetate) [13].

The free volume in a polymer can also be determined, though not directly measured, using an equation of state approach. One such equation of state is derived from the Simha–Somcynsky lattice-hole theory (S–S eos) [14,15]. This theory describes a macromolecular liquid as a collection of cells of equal volume arranged in a periodic lattice with coordination number $z = 12$, each one of which is either occupied or unoccupied. The S–S eos is based on the principle of corresponding states [16] whereby one equation, or set of coupled equations, form the equations of state in terms of reduced variables. The mechanics of this approach will be described in more detail later in this paper. Links between the specific free volume determined in this way and the local free volume from PALS have been explored extensively; see for example [17,18]. By comparing these two measures it has been suggested that the number of holes, as measured by PALS, can be calculated [19]. More recently, the free volume from the S–S eos approach has been used in more detailed models of structural relaxation by Dlubek et al. [13].

This paper will deal with the temperature dependence of free volume in a series of poly(*n*-alkyl methacrylate)s and compare this with relaxation data. The polymer samples used have previously been studied extensively by the experimental polymer physics group of the University of Halle (Germany) employing conventional (DSC) and temperature modulated differential scanning calorimetry (TMDSC), broadband dielectric spectroscopy, and other methods [20–24]. Poly(*n*-alkyl methacrylate)s are an ideal system for a study of this nature as their relaxation characteristics can be systematically altered by changing the side-chain length. Of particular interest in this respect is the frequency of dielectric relaxations at the crossover temperature: this frequency becomes lower the more the side-chain length is increased [20,21]. Poly(*n*-alkyl methacrylate)s are also an interesting system to study in material terms alone as they and their derivatives are finding applications in such fields as non-linear optics and energy storage [22]. This work goes beyond previous PALS studies on poly(*n*-alkyl methacrylate)s, for example Malhotra and Pethrick [25] and Li et al. [26], by combining PALS and PVT S–S eos to characterize completely the structure of the free volume. Moreover, the dispersion of hole sizes leading to a dispersion in the various lifetimes is analysed. The structural (α-)relaxation data from Refs. [20–24] are analysed in order to test the validity and limits of the Cohen–Turnbull free volume theory. Moreover, we discuss whether the crossover from the low-temperature α-relaxation to the high-temperature a-relaxation has an effect on the hole volume expansion.

2. Experimental section

2.1. Samples

A series of poly(*n*-alkyl methacrylate)s, $[-CH_2-C(CH_3)(COOR')-]_n$ where $R' = C_CH_{2C+1}$ is the alkyl part of the side-chain and the index '*C*' gives the number of carbon atoms in the alkyl part, were investigated. The series contains: poly(methyl methacrylate), PMMA, $C = 1$; poly(ethyl methacrylate), PEMA, $C = 2$; poly(*n*-propyl methacrylate), PPMA, $C = 3$; poly(*n*-butyl methacrylate), PBMA, $C = 4$; poly(*n*-hexyl methacrylate), PHMA, $C = 6$. The samples were kindly provided by Dr. M. Beiner, Universität Halle, and, as already mentioned, characterized in previous works [20–24]. The molar masses of the repeat units, M_{rep}, and the weight average molecular masses, M_W, are shown in Table 1. Table 2 contains the glass transition temperature from DSC and further parameters characteristic of the segmental dynamics.

2.2. Positron lifetime experiments

The PALS measurements were performed using a fast–fast coincidence system [3] with a time resolution of 290 ps (FWHM, ^{22}Na source). Two identical samples of 1 mm thickness were sandwiched around a 1×10^6 Bq positron source: ^{22}NaCl, deposited between two 8 μm thick Kapton foils. To prevent sticking of the source to the samples at higher

Table 1
Sample characterisation and volume parameters from PVT data

Quantity	±[a]	PMMA	PEMA	PPMA	PBMA	PHMA
M_{rep}, g/mol		100	114	128	142	170
M_W, kg/mol		86	154	283	160	178
T_g (PVT), K	3	376	334	n/d	n/d	268
T_0' (PVT), K	5	244	222	218	207	179
E_g, 10^{-4} cm^3 g^{-1} K^{-1}	0.08	2.11	3.81	n/d	n/d	4.40
E_r, 10^{-4} cm^3 g^{-1} K^{-1}	0.04	4.99	5.97	6.11	6.17	6.80
$V(T_g)$, cm^3 g^{-1}	0.002	0.868	0.893	0.913	0.946(4)	0.972
$V_{occ}(T_g)$, cm^3 g^{-1}	0.002	0.804	0.829	0.855	0.887	0.914
$V_f(T_g)$, cm^3 g^{-1}	0.002	0.064	0.064	0.058	0.060(4)	0.058
$h(T_g)$	0.002	0.073	0.072	0.064	0.063(4)	0.059
$V_{occ}(0)$, cm^3 g^{-1} [b]	0.001	0.798(2)	0.822	0.848	0.880	0.907(2)
V^*, cm^3 g^{-1}	0.001	0.842	0.868	0.895	0.929	0.958
T^*, K	50	11900	10600	10450	10300	9200
P^*, MPa	10	1050	880	860	860	n/d
M_0, g/mol	0.4	37.4	38.3	37.6	35.7	n/d
v_{SS} (T_g), Å^3	0.5	50	52.7	53.4	52.6	n/d
$E_{f,g}$, 10^{-4} cm^3 g^{-1} K^{-1}	0.05	1.37	2.90	n/d	n/d	3.57
$E_{f,r}$, 10^{-4} cm^3 g^{-1} K^{-1}	0.02	4.81	5.66	5.98	6.00	6.53
$E_{occ,g}$, 10^{-5} cm^3 g^{-1} K^{-1}	0.05	7.33	6.04	n/d	n/d	8.32
$E_{occ,r}$, 10^{-5} cm^3 g^{-1} K^{-1}	0.03	1.62	1.90	2.03	2.24	2.73

[a] Uncertainties given are mean values for the material series. If the error for one particular measurement is unusually large, the error for the last significant figure is given in brackets next to the relevant measurement.
[b] From plot of V_{occ} vs. T extrapolated from above T_g down to absolute zero.

temperatures, each sample was covered with an additional foil of 8 μm thick Kapton. Source corrections, due to positrons annihilating in the salt and Kapton foils, were determined from the defect-free aluminium reference measurements. These source corrections were: 8.5% at 343 ps and 0.5% at 2.7 ns. The time resolution function used for the final fitting

Table 2
Free volume parameters from PALS data and other literature parameters used in this work

Quantity	±[a]	PMMA	PEMA	PPMA	PBMA	PHMA
T_g (PALS), K[b]	5	382	331	315	307(10)	224
T_g (DSC), K[c]	3	379	343	324	298	253
τ_3 (295), ns	0.05	2.02	2.18	2.23	2.43	2.67
T_0' (PALS), K	20	296	210	215	166	169
T_0, K[c]		371	304	285	256	215
$B_\alpha/\ln 10$, K[c]		366	361	359	361	389
T_+, K[d]		450	380	n/a	323	282
$\log(\omega)$, rad s^{-1} [d]		10.8	8.3	7.6	7.6	6.8
$\langle v_h \rangle$ (295), Å^3	5	79	88	91	99	119
$\langle v_h \rangle$ (T_g), Å^3	5	90	91	95	103	52
e_{hg}, Å^3/K[e]	0.03	0.13	0.10	0.25	0.30	0.28
e_{hr}, Å^3/K[e]	0.04	1.03	0.75	0.96	0.73	0.94
α_{hg}, 10^{-3} K^{-1} [e]	0.4	1.4	1.1	2.6	2.9	5.5
α_{hr}, 10^{-3} K^{-1} [e]	0.6	11.5	8.2	10.0	7.1	18.1
N_h', 10^{21} g^{-1} [f]	0.04	0.54	0.74	0.66	0.86	0.66
V_{f0}, cm^3/g[f]	0.006	0.017	−0.004	−0.006	−0.032	−0.002
N_h', 10^{21} g^{-1} [h]	0.04	0.57	0.77	0.68	0.86	0.69
$V_{occ} + V_{f0}$, cm^3/g[h]	0.005	0.820(8)	0.821	0.847	0.856(6)	0.909
N_h', 10^{21} g^{-1} [g]	0.01	0.67	0.70	0.62	0.65	0.64
$N_h = N_h'/V(T_g)$, nm^{-3} [g]	0.04	0.78	0.79	0.67	0.69	0.66
γV_f^*, cm^3/g	0.03	0.38	0.37	0.59	0.53	0.17
ΔV, cm^3/g	0.003	0.062	0.052	0.038	0.028	0.043

[a] Uncertainties given are mean values for the material series. If the error for one particular measurement is unusually large, the error for the last significant figure is given in brackets next to the relevant measurement.
[b] Determined from linear least-square fits of straight lines to $\langle v_h \rangle$ vs. T above and below T_g, as shown in Fig. 9.
[c] From Ref. [21].
[d] From Ref. [48] α-relaxation, temperatures between T_g and T_+ (PMMA, PEMA, PBMA). Fitted from data in Ref. [21] (PPMA, PHMA).
[e] Subscripts 'g' and 'r' on expansivities and coefficients of expansion refer to the glassy and rubbery phases, respectively.
[f] From linear least-square fits to plots of V_f vs. $\langle v_h \rangle$.
[g] From linear least-square fits to plots of V_f vs. $\langle v_h \rangle$ constrained to pass through the origin.
[h] From linear least-square fits to plots of V vs. $\langle v_h \rangle$.

procedure was determined consisting of the sum of three Gaussian functions.

The temperature of the samples, placed in a vacuum chamber, was varied, at maximum between 140 and 480 K, in steps of 10 K with an uncertainty of ±1 K. For some of the samples the heating scan was followed by a cooling scan in steps of 10 K down to 293 K. Since no hysteresis was observed in the lifetimes, these results will not be discussed.

2.3. PVT experiments

The PVT experiments [27] were carried out by means of a fully automated GNOMIX high-pressure dilatometer. The data were collected in the range from room temperature to 250 °C in steps of 10 K. At each temperature the material was pressurized from 10 to 200 MPa. The specific volumes for atmospheric pressure were obtained by extrapolating the values for 10–30 MPa in steps of 1 MPa according to the Tait equation using the standard GNOMIX PVT software. The instrument is able to detect changes in specific volume as small as 0.0002 cm^3/g with an absolute accuracy of 0.002 cm^3/g. The data obtained in a cooling run after the heating showed a disappearing small hysteresis when compared with the heating data and are therefore not discussed. The densities of the samples at room temperature were determined by means of an Ultrapycnometer 1000 (Quantachrome) with an accuracy of 0.03%.

3. Results and discussion

3.1. Specific volume and S–S eos analysis of PVT data

Fig. 1 shows the temperature dependence of the specific volume, V, extrapolated from PVT measurements to ambient pressure ($P \sim 0$ MPa), of the series of poly(n-alkyl methacrylate)s. The glass transition is marked, as is usually reported, by a sudden increase in expansivity. For a given temperature the specific volume increases with increasing C-number. The data for PHMA were reconstructed from fit values in the paper of Rogers and Mandelkern [28]. This should be treated with a certain degree of caution as the molecular weights are not given in the paper and so it is unclear as to whether they are consistent for the materials tested here. The specific volume variation for the other materials in the series shows a good agreement between that of Rogers and Mandelkern and ours, which is an indication that their data may be valid for use here. The quality of the linear fits to the data to give the specific thermal expansivities $E_g = dV/dT$ ($T < T_g$) and $E_r = dV/dT$ ($T > T_g$) are very good, the fitted values are listed in Table 1. The values of E_g, insofar as we have them, increase with increasing C-number, as do those of E_r.

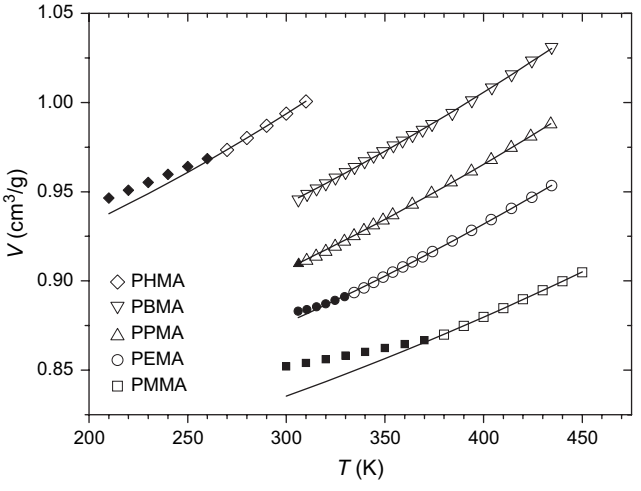

Fig. 1. Specific volume, V, of poly(n-alkyl methacrylate)s as a function of temperature, T, at ambient pressure. Symbols: experimental data. Line: fits to the data above T_g (empty symbols) according to Eq. (2). Data for PHMA reconstructed from fit values in Rogers and Mandelkern [28].

The PVT data were next analysed using the S–S eos theory [14,15]. As mentioned in Section 1, this theory describes a macromolecular liquid as a collection of cells of equal volume arranged in a periodic lattice with coordination number $z = 12$, each one of which is either occupied or unoccupied. The theory models the chains as being composed of equivalent segments (mers of the S–S lattice denoted as s-mers which are not necessarily monomeric units), each one of which moves in the potential field of its intermolecular neighbours.

Each cell in the occupied fraction contains the van der Waals volume of an s-mer, referred to above as a 'segment', as well as an inherent free volume. For a sample containing N molecules, each consisting of n chemical repeating units (n-mers) with molecular weight M_{rep}, the following relationship applies: $sM_0 = nM_{rep}$. The occupied fraction, y, consisting of sN cells, can be expressed as $y = sN/(sN + N_h^{SS})$, where N_h^{SS} is the number of unoccupied cells and $h = 1 - y$ is the hole free volume fraction defined according to this theory. These unoccupied cells constitute the hole free volume in the liquid where the free volume (hole) fraction is defined as $h = V_f/V$, V_f being the specific hole free volume. The specific occupied volume defined according to the S–S eos is $V_{occ} = yV = V - V_f$.

Two expressions are constructed by using the above assumptions to express the partition function: the first follows from the relationship between pressure and Helmholtz free energy, $P = -(\partial F/\partial V)_T$:

$$\frac{\tilde{P}\tilde{V}}{\tilde{T}} = \left[1 - y\left(2^{1/2}y\tilde{V}\right)^{-1/3}\right] + \frac{y}{\tilde{T}}\left[2.002\left(y\tilde{V}\right)^{-4} - 2.409\left(y\tilde{V}\right)^{-2}\right] \quad (1)$$

the second is obtained by minimising the Helmholtz free energy with respect to y, $(\partial F/\partial y)_{V,T} = 0$. $\tilde{P} = P/P^*$ etc., where P^* is the reduced pressure for the system under consideration.

The two equations define the $\tilde{P}$–$\tilde{V}$–$\tilde{T}$ surface together with the occupied fraction for any molecular liquid. It was shown by Utracki and Simha [29] that the two equations can be replaced in the temperature and pressure ranges $\tilde{T} = 0.016$–0.071 and $\tilde{P} = 0$–0.35 by the universal interpolation expression:

$$\ln \tilde{V} = a_0 + a_1\tilde{T}^{3/2} + \tilde{P}\left[a_2 + \left(a_3 + a_4\tilde{P} + a_5\tilde{P}^2\right)\tilde{T}^2\right] \quad (2)$$

where $a_0 = -0.10346$, $a_1 = 23.854$, $a_2 = -0.1320$, $a_3 = -333.7$, $a_4 = 1032.5$ and $a_5 = -1329.9$. A similar expression is written

for h in terms of $\tilde{T}$ and $\tilde{V}$ in the same paper, but there is presently no universal relationship for the h-function in the glassy state. Eq. (2) is useful as it gives an analytical expression, which can be fitted to experimental data in order to determine the scaling parameters for use in Eq. (1).

The method for calculating V_{occ} and V_f is as follows:

1. A non-linear least-squares fit of Eq. (2) to zero pressure volume data ($P = 0$, determined via an extrapolation of a Tait equation fit to the data in the range 10–30 MPa) is carried out to determine T^* and V^*. Since Eq. (2) is valid for the liquid phase only, the data are fitted in the temperature range from $T_g + 10$ °C to 250 °C.
2. Using the values of T^* and V^* from step 1, a second fit was performed, this time using all of Eq. (2) for the measured PVT field above the pressure-dependent T_g and in the range 0–200 MPa, which allowed P^* to be calculated.
3. Solving Eq. (1) numerically using experimental PVT data and P^*, V^* and T^* determined from the previous step, it is possible to calculate y and therefore h at all measured temperatures and pressures. As the positron measurements are made in a vacuum, determining h at zero pressure is a valid approximation for comparison. The specific occupied and free volumes, V_{occ} and V_f, respectively, are then calculated as detailed above by multiplying the relevant fraction by the total specific volume.

It can be seen in Fig. 1 that the scaling parameters (shown in Table 1), used in Eq. (2), give an excellent approximation to the experimental data at atmospheric pressure above T_g. T^* decreases with increasing C-number; as noted by Wilson and Simha [30], a decrease in T^* suggests an increase in effectively external degrees of freedom with increasing temperature. This seems to fit the view of those poly(n-alkyl methacrylate)s with longer side chains (higher C-number) being more molecularly mobile, leading to lower T_gs. Values of V^* increase with increasing C-number; indeed, a plot of V^* against the van der Waals volume of a monomer unit agrees very well with a plot of the function V^* (cm^3/mol) = $1.45(\pm0.01)V_W + 3.88(\pm3.82)$ reported by Simha and Carri [31]. Once the reducing parameters are known, the mass of an s-mer, M_0, can be calculated [29]. The product of M_0 and the specific occupied volume at T_g (divided by N_A) is the volume of an unoccupied S–S cell at this temperature, v_{SS}. Values of M_0 and v_{SS} are shown in Table 1.

The specific free volume, $V_f = hV$, is shown as a function of temperature at $P = 0$ in Fig. 2. As can be seen, this plot is as would be expected with the free volume increasing linearly with temperature but with a discontinuity in the linear expansivity at T_g. The specific thermal expansivity below T_g, $E_{f,g} = dV_f/dT$ ($T < T_g$) (Table 1) increases as C-number increases from 1 to 6. Like the expansivity of the total specific volume, the expansivity of the specific free volume above T_g, $E_{f,r} = dV_f/dT$ ($T > T_g$), increases with increasing C-number. Linearly extrapolating the V_f data from the rubbery state down to zero gives the temperature T_0' (PVT), values are displayed in Table 1. In a simplistic picture of free volume and mobility T_0' (PVT) should be equal to the temperature at which (the extrapolated) molecular mobility disappears, known as the Vogel temperature, T_0. Reasons for this not being the case (T_0 values are displayed in Table 2) will be discussed later. The specific expansivity of the occupied volume is an order of magnitude lower than that of the free volume and decreases above T_g, but is still non-negligible (Fig. 3), values are given in Table 1.

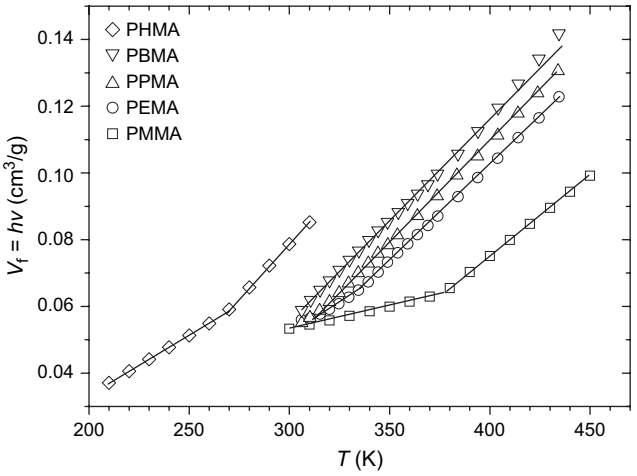

Fig. 2. Specific free volume, V_f, of poly(n-alkyl methacrylate)s as a function of temperature, T, at ambient pressure. Solid lines are linear fits above and below T_g.

Fig. 4 shows the specific volume, V, and the specific occupied volume, V_{occ}, and Fig. 5 shows the specific free volume, V_f, of poly(ethyl methacrylate) as a function of temperature for pressures between 0 and 200 MPa. It can be seen that with increasing pressure at all temperatures all three of these are compressible. The glass transition temperature increases from 334 to 370 K as P increases from 0 to 200 MPa. With increasing pressure, the thermal expansivity of V and V_f above T_g decreases in line with previous observations. Interestingly, the thermal expansion of V_{occ} is almost independent of the pressure below in the rubbery as well in the glassy state.

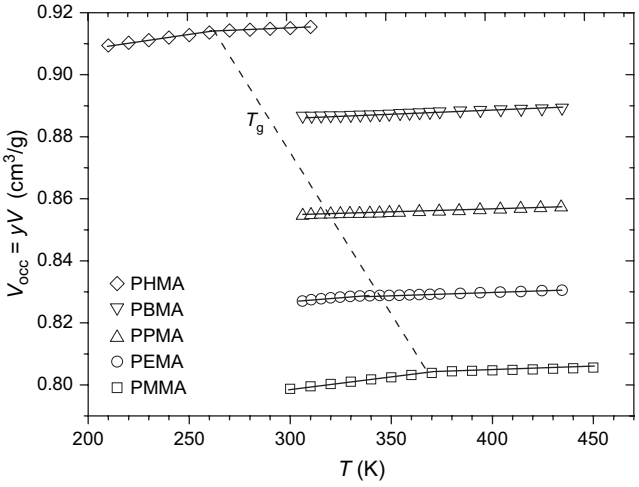

Fig. 3. Specific occupied volume, V_{occ}, of poly(n-alkyl methacrylate)s as a function of temperature, T, at ambient pressure. Solid lines are linear fits above and below T_g. Dashed line approximately follows the T_gs.

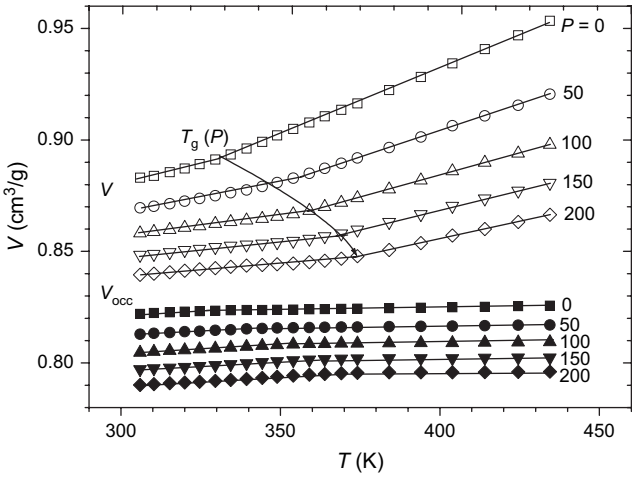

Fig. 4. Specific volume (empty symbols), V, and specific occupied volume (filled symbols), V_{occ}, of poly(ethyl methacrylate) as a function of temperature at a series of pressures, given in MPa. Lines are shown to guide the eyes and $T_g(P)$ is indicated for V_{occ}.

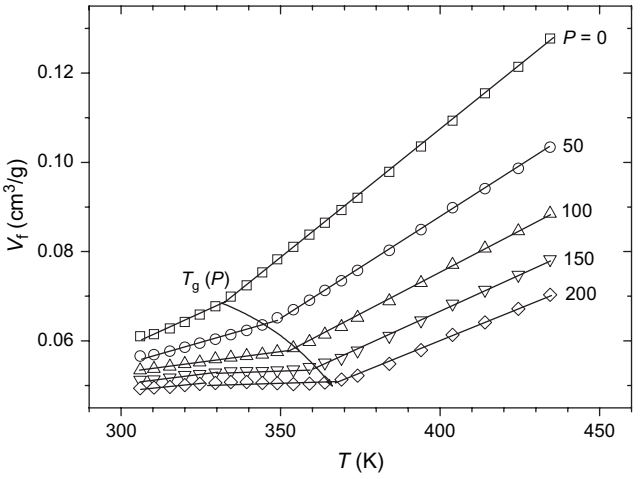

Fig. 5. Specific free volume (empty symbols), V_f, poly(ethyl methacrylate) as a function of temperature at a series of pressures, given in MPa. Lines are shown to guide the eyes and $T_g(P)$ is indicated.

3.2. Positron lifetime spectra analysis

In molecular matter positrons can annihilate with electrons directly, or can form a bound state with an electron, the positronium atom (Ps), and subsequently annihilate with this bound electron or with an auxiliary one. A given number of positrons annihilating from a single state will have their (individual) lifetimes distributed according to Eq. (3),

$$P_i(t) = \frac{1}{\tau_i}\exp\left(\frac{-t}{\tau_i}\right) \tag{3}$$

where $P_i(t)$ gives the probability of a positron in the given state, i, annihilating in the time interval between t and $t+\delta t$ after the birth of positron. The mean lifetime of a positron in the given state is τ_i. Lifetime spectra have conventionally been described as a sum of three decay components like that given in Eq. (3): $S(t) = \sum I_i P_i(t)$, $i = 1, 2, 3$, where I_i is the relative intensity (fraction of annihilation events) of the ith component, $\sum I_i = 1$. The three components are interpreted as being due to annihilation of the *para* state of Ps (p-Ps, $\tau_1 \sim 125-200$ ps), free (e^+ not Ps) positrons ($\tau_2 \sim 370-450$ ps), and the *ortho* state of Ps (o-Ps, $\tau_3 = 1.5-4$ ns) [3,4]. In vacuum o-Ps has a mean lifetime of 142 ns but this is reduced in amorphous polymers to the value quoted by the positron annihilating with an electron other than its bound partner and of opposite spin (pick-off annihilation). Conventional analysis involves a non-linear, least-squares fit of the equation:

$$S_{exp}(t) = N[S(t) \otimes R(t)] + B \tag{4}$$

where $R(t)$ is the resolution function of the spectrometer, N is the total number of counts and B is a background count level. The Tao–Eldrup equation [5,32] links a single characteristic free volume hole size to a single characteristic lifetime of o-Ps. This semi-empirical equation assumes a spherical hole symmetry and that o-Ps is a point particle in an infinite potential well, annihilating via pick-off in an electron-containing layer of thickness δr. The o-Ps lifetime is given by:

$$\tau_{po} = 0.5\ \text{ns}\left[1 - \frac{r_h}{r_h+\delta r} + \frac{1}{2\pi}\sin\left(\frac{2\pi r_h}{r_h+\delta r}\right)\right]^{-1} \tag{5}$$

where $\tau_{po} = \tau_3$ is the o-Ps 'pick-off' lifetime, $\delta r = 1.66$ Å and r_h is the radius of the hole in which the o-Ps is located. In real systems it is anticipated that fitting to discrete lifetimes will be something of a crude approximation as there is likely to be a distribution of hole radii giving a distribution of lifetimes. To account for this the program LT9 [33,34] is used to fit lifetimes τ_i with distributions, mimicking the hole size (and shape) distributions. The assumption of a one-to-one relationship between o-Ps lifetime distributions and hole size distributions has been discussed previously and found to be valid due to Anderson localization meaning that a Ps samples a single hole before decaying [35]. For extensive discussions on lifetime data analysis, particularly taking lifetime distributions into account, see Refs. [36,37]. Using LT9, the annihilation rates are assumed to be log-normally distributed; this choice of distribution is supported by previous analyses using CONTIN where a fully continuous distribution of lifetimes is allowed [33]. The outputs from LT9 in distribution mode are: the intensity of each lifetime, I_i; the mean lifetime of each channel, τ_i; and the standard deviation of the lifetimes from each component, σ_i.

3.3. Results of PALS analysis

When analysing PALS data, choices have to be made as to restrictions in the fitting parameters. The analysis scheme in the present paper has followed that adopted in Ref. [37]. To summarise: τ_1, τ_2, τ_3, σ_2, and σ_3 are unconstrained; $\sigma_1 = 0$; I_1/I_3 was constrained to be 1/3. The results of alternative

analyses will not be presented, but the similarity in the variation of parameters with constraints to those previously reported [37] increases confidence in the final analysis presented here.

Values obtained for τ_1 (not shown) are constant for the temperature ranges measured and fall in the range 0.15–0.20 ns, τ_2 and σ_2 (not shown) show similar behaviour to that observed in Ref. [37]: they both (weakly) increase with temperature with a distinct positive step in the gradient at T_g. τ_2 varies between 0.350 and 0.400 ns and σ_2 values lie in the region 0.07–0.14 ns. The mean *o*-Ps lifetimes, τ_3s, are shown in Fig. 6. A glass transition signifier (denoted as 'T_g' on plot) is marked by a sudden increase in the gradient of τ_3 against T with constant gradient both above and below. It can also be seen that at room temperature (taken as 295 K) τ_3 increases with increasing *C*-number; from 2.02 ± 0.01 ns for PMMA to 2.67 ± 0.09 ns for PHMA (Table 2), this is caused by increasing free volume and the physical explanation for this will be discussed later, along with the other hole free volume data. The data for PMMA are broadly similar to those observed in PALS experiments by Schmidt and Maurer [38], although some differences do exist. They found T_g to be 366 K as opposed to 382 ± 2 K found by us (see Table 2); a value of 375 K can be estimated from PALS experiments reported by Malhotra and Pethrick [25].

Fig. 7 shows, as an example, the mean dispersion in τ_3, σ_3, as a function of temperature for two different fitting schemes for PMMA. It can be seen that the inclusion of a dispersion in τ_2 clearly reduces the final fitted values of σ_3. This effect has been observed before [37] although in that work the difference was less. The values of σ_3 when $\sigma_2 > 0$ agree with those found for PMMA by Wang et al. [39] who used the distribution analysis program MELT.

The intensities of the *o*-Ps lifetimes, I_3, are shown in Fig. 8, where a common pattern can be observed despite there being a large amount of scatter in the data points. It can be seen that generally the intensity increases with both temperature and

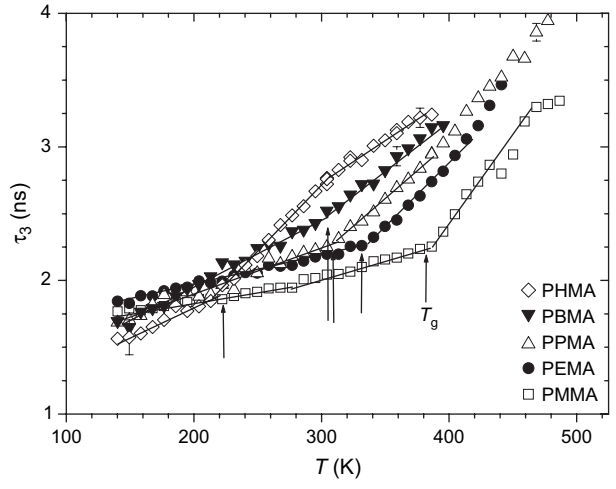

Fig. 6. Mean lifetime of the *o*-Ps component of the lifetime spectra, τ_3, for the series of poly(*n*-alkyl methacrylate)s as a function of temperature, T, at zero pressure. Representative error bars are shown for PHMA and PBMA; for other series the error bars are similar of size to data points. The arrows indicate the glass transitions.

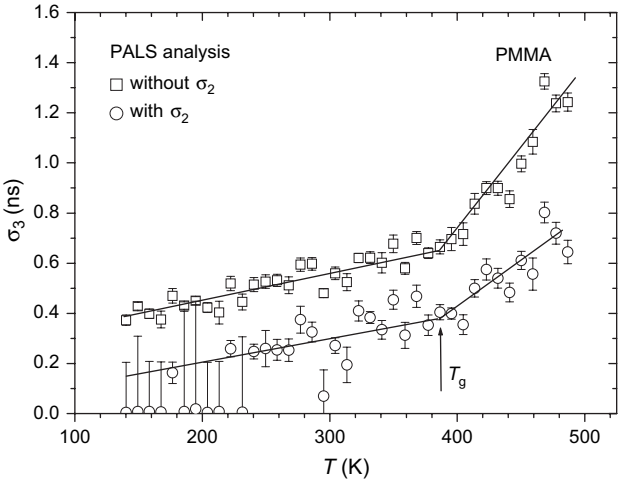

Fig. 7. Mean dispersion of the *o*-Ps component of the lifetime spectra, σ_3, for poly(methyl methacrylate) as a function of temperature, T. The results of two fitting schemes are shown: allowing a dispersion in τ_2 ($\sigma_2 > 0$, circles), having a discrete τ_2 component ($\sigma_2 = 0$, squares). σ_1 was assumed to be always zero. Lines shown are non-linear least-square fits of a straight line.

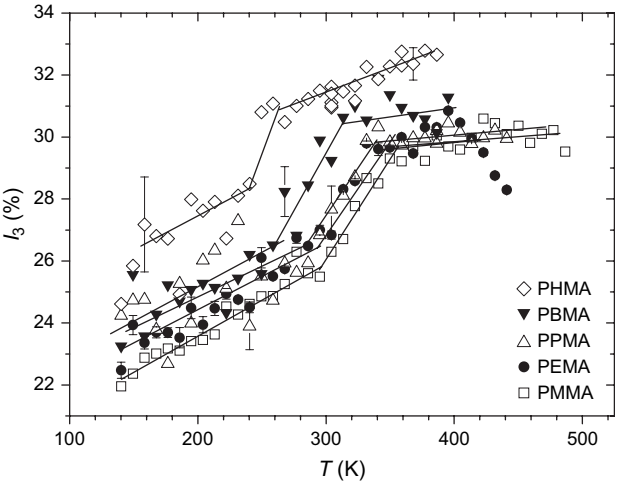

Fig. 8. Intensities of the *o*-Ps components of the lifetime spectra, I_3, for the series of poly(*n*-alkyl methacrylate)s. To avoid over-clustering of the graph, representative error bars are drawn.

C-number. Furthermore, a jump in intensity is observed in all the materials' plots. Similar data have been presented previously [25] where less uniform behaviour is observed; the intensity variously increases and decreases, depending on the material. Taking the data for PMMA, Malhotra and Pethrick [25] report a sudden increase from ~31% to ~37% at T_g, whereas we see an increase from ~25% to ~29% over the range 80–30 K below T_g.

3.4. Mean hole size and hole size distribution

The commonly used semi-empirical Tao–Eldrup equation (Eq. (5)) links an *o*-Ps 'pick-off' lifetime (or, equivalently, annihilation rate) to a free volume hole size. In a situation where a single mean lifetime is obtained from a fit to a PAL spectrum it is therefore a simple operation to obtain a mean hole volume corresponding to that lifetime. As mentioned

above, the program LT9 can also be operated to assume a log-normal distribution of the value $\alpha_i(\lambda)\lambda$ where $\alpha_i(\lambda)$ is the annihilation rate for the ith annihilation channel. The maximum of this distribution, λ_{i0}, and its standard deviation, $\sigma_i(\lambda)$, is related to the mean o-Ps lifetime, τ_3, and its standard deviation, σ_3, by the relations $\tau_3 = \exp[\sigma_3(\lambda)^2/2]/\lambda_{30}$ and $\sigma_3 = \sigma(\tau_3) = \tau_3[\exp(\sigma_3(\lambda)^2 - 1]^{0.5}$. From these distributions it is possible to calculate the hole radius probability distribution, $n(r_h) = -\alpha_3(\lambda)\mathrm{d}\lambda_3/\mathrm{d}r_h$, and from this the volume-fraction hole size distribution, $g(v_h) = n(r_h)/4\pi r_h^2$, and the number-fraction hole size distribution, $g_n(v_h) = g(v_h)/v_h$. For details of these calculations, see Dlubek et al. [37]. It has been suggested that positrons sample holes in a volume-weighted manner [37,40], preferentially annihilating in larger holes. This means that $g_n(v_h)$ is no longer a true representation of the number-fraction hole size distribution as each point on that curve is sampled proportionally according to its volume, v_h. It is therefore necessary to calculate and consider $g_n(v_h)$ weighted with $1/v_h$, $g_n(v_h)^* = g_n(v_h)/v_h$. Following the calculation of these distributions and their mean values, $\langle v_h\rangle^*$, and standard deviations (calculated numerically), σ_h^*, it was found that considerable scatter existed in the final values for $g_n(v_h)^*$. To compensate this, in the final analysis, the values of σ_3 obtained from the PAL spectra were fitted to straight lines against temperature. The fitted values thus obtained over the full temperature range were used to calculate $\sigma_3(\lambda)$ and thereafter the various hole volume distributions. For convenience, the quantities $\langle v_h\rangle^*$ and σ_h^{*2} are renamed as $\langle v_h\rangle$ and σ_h^2: the mean and the variance of the *true* number-weighted hole size distribution.

Fig. 9 shows $\langle v_h\rangle$ as a function of temperature for the full series of poly(n-alkyl methacrylate)s. The straight lines are due to linear least-square fits to the data and from these fits T_gs, thermal expansivities, $e_h = \mathrm{d}\langle v_h\rangle/\mathrm{d}T$, and hole volumes at room temperature ($\langle v_h(295)\rangle$) and T_g ($\langle v_h(T_g)\rangle$) can be calculated (all the values are in Table 2). Firstly, it can be seen that $\langle v_h\rangle(295)$ increases with increasing C-number; the effect of $\langle v_h\rangle$ increasing with increasing side-chain length has been observed previously [41]. The appearance of sterical hindrances as a result of the extra side-chains prevents effective packing of the polymer molecules. This is seen as the increase in hole size. The increase in local free volume allows a higher molecular mobility indicated by the lowering of T_g and a general increase in the frequency of α-relaxation at a given temperature.

At low temperatures, o-Ps is trapped in local free volumes within the glassy matrix and τ_3, and hence $\langle v_h\rangle$ shows the mean size of static holes. The averaging occurs over the hole sizes and shapes. The slight increase of $\langle v_h\rangle$ with temperature mirrors the thermal expansion of free volume in the glass due to the anharmonicity of molecular vibrations and local motions in the vicinity of the holes. In the rubbery phase, $T > T_g$, the molecular and segmental motions increase rapidly, resulting in a steep rise in the hole size with temperature. Above T_g, $\langle v_h\rangle$ represents an average value of the local free volumes whose size and shape fluctuate in space and time, provided the timescale of a typical segmental relaxation is greater than the mean o-Ps lifetime.

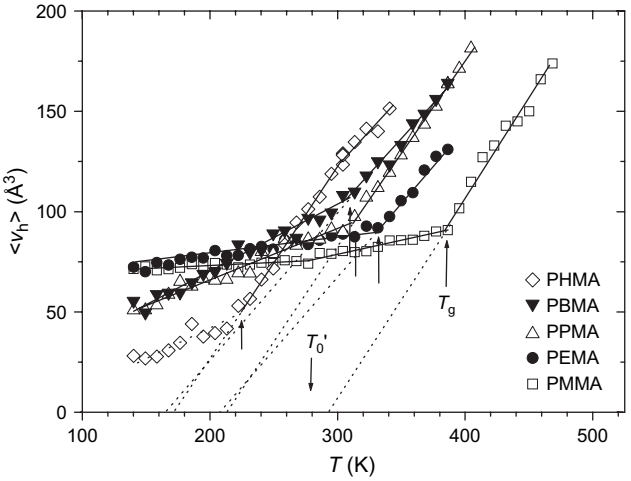

Fig. 9. Mean hole volume as measured by PALS and analysed according to protocol outlined in the text. T_g denotes the glass transition. Straight lines are due to linear fits.

Values calculated for thermal expansivities, e_h, and coefficients of thermal expansion, $\alpha_h = (1/\langle v_h(T_g)\rangle)\mathrm{d}\langle v_h\rangle/\mathrm{d}T = e_h/\langle v_h\rangle(T_g)$, are shown in Table 2. There is a tendency of the thermal expansivity of the glass, $e_{h,g}$, to increase with increasing C-number for $C > 2$ (Fig. 9 and Table 2). Beiner et al. [42] observed in X-ray scattering experiments an increasing tendency of nanophase separation with increasing length of the alkyl group. From dielectric relaxation experiments these authors concluded on a main chain independent polyethylene-like α-relaxation interpreted as hindered glass transition in self-assembled alkyl nanodomains. This relaxation is reported to have maxima in the shear loss modulus curves ($\omega = 10\ \mathrm{rad\ s^{-1}}$) at $T \approx 150$ K ($C = 3$) to ≈170 K ($C = 6$) [42]. Probably, this additional transition causes the extraordinarily high value of $e_{h,g}$ for the higher poly(n-alkyl methacrylate)s.

Linear extrapolation of the mean hole volume from the rubbery state down to zero hole volume gives T_0'(PALS) (Fig. 9 and Table 2). The values obtained from the fits to $\langle v_h\rangle = \langle v_h\rangle^*$ are closest to those obtained from fits to V_f (given in Table 1 as T_0'(PVT)) although the difference is still significant for PMMA.

Along with the Vogel temperature T_0, the relaxations of a polymer are characterized by the crossover (or onset) temperature, T_+ (values for the poly(n-alkyl methacrylate)s are shown in Table 2). T_+ is marked in a dielectric relaxation spectrum by the splitting of the high-temperature a-relaxation peak into the sum of the (secondary) β-relaxation and the slower, low-temperature α-relaxation. α and a are characterized by different sets of VFT parameters, sometimes the VFT behaviour goes over into an Arrhenius behaviour. It is believed that at T_+ the polymer goes over from a ''cold'' liquid characterized by a dynamic heterogeneity and cooperative rearranging of monomeric units to a ''warm'' liquid characterized by vanishing dynamic heterogeneity, i.e. all monomeric units are dynamically equivalent and can move non-cooperatively [43].

There is the interesting question whether the free volume expansion shows any response to the change in the structural dynamics at T_+. It is known that at higher temperatures the

expansion of the *o*-Ps lifetime, τ_3, shows a levelling-off. In the materials in this study only PMMA shows the onset of this effect at 470–480 K (''knee'' in τ_3 in Fig. 6). The nature of this effect is under discussion. One possible interpretation, discussed by Ngai et al. [44], is that the knee mirrors the vanishing of dynamic heterogeneity in the structural relaxation and should correlate with T_+. For PMMA T_+ appears, however, at 450 K (Table 2) and the other polymers show no specific feature of the PAL spectra in coincidence with the dynamic crossover at T_+. Probably, and as discussed in detail by Dlubek et al. [36,37,45], the levelling-off in τ_3 is due the decrease of the relaxation time of structural relaxation which comes at high temperature in the magnitude of the *o*-Ps lifetime. Indeed, Bartoš et al. have discussed this effect from a phenomenological perspective [46,47], noting that for a number of glass-formers this is the point at which the time-scales of the structural relaxation and positron annihilation become commensurate. This occurs for the higher poly(*n*-alkyl methacrylate)s investigated in this work only at temperatures above the range of the current experiments.

3.5. Calculating the hole density

The density of the holes in a polymer sampled by positrons can be estimated using one of the relations [18]

$$V_\mathrm{f} = N'_h \langle v_h \rangle \tag{6}$$

$$V = V_\mathrm{occ} + N'_h \langle v_h \rangle \tag{7}$$

where N'_h is the number of holes per mass unit. Here, the free volume is expressed by $N'_\mathrm{h}\langle v_\mathrm{h}\rangle$ and Eq. (6) assumes that the free volume as detected by PALS is the same as the free volume $V_\mathrm{f} = hV$ estimated from the S–S eos. Eq. (7) can be considered as an empirical, model-free, relation.

Fig. 10 shows plots of V_f vs. $\langle v_\mathrm{h}\rangle$ for the entire series of materials. The data shown are from above T_g. For all of the materials, Eq. (6) is fitted to the data. It is found that, as with previous work, the plots are linear above T_g which implies a constant or very slowly varying N'_h. Two fits were performed: one, a linear least-squares fit giving the $V_{\mathrm{f}0}$ (that is the intercept on the *y*-axis) values and N'_h values listed in Table 2; and another, because $V_{\mathrm{f}0}$ was found to be approximately equal to zero, a linear least-squares fit constrained to pass through the origin. The N'_h values resulting with this constraint are also listed in Table 2. Fig. 11 shows plots of V vs. $\langle v_\mathrm{h}\rangle$ for the series of materials, the lines are the results of least-square fits of Eq. (7) to the data. Values of V_occ and N'_h from these fits are listed in Table 2. It can be seen that the values from Eq. (7) correspond to those from unconstrained fits of Eq. (6). The fitted values of V_occ include in this case the value $V_{\mathrm{f}0}$. If one compares $V_\mathrm{occ} = V_\mathrm{occ}(\mathrm{fit}) - V_{\mathrm{f}0}$ (from values in Table 2) with $V_\mathrm{occ}(0)$ (Table 1) from S–S eos, derived by extrapolating V_occ vs. T to 0 K, it can be seen that the two sets of values agree with each other to within statistical scatter.

The order of magnitude of the values for N'_h calculated here are similar to those reported before. For a direct comparison, Schmidt and Maurer [38] have calculated N'_h for PMMA using the same method as in this paper and an equation equivalent to Eq. (7). They obtained a value of $N'_\mathrm{h} = 0.62 \times 10^{21}$, compared with the value reported here of $0.57 \pm 0.04 \times 10^{21}$. Bearing in mind the level of uncertainty in the measurement, these seem to agree well.

The number of holes per unit volume, N_h, is given by $N_\mathrm{h} = \rho N'_\mathrm{h}$. Using this equation in conjunction with values of N'_h already calculated, the number of holes per unit volume at T_g are calculated and found to be of the order of 0.6–1 nm^{-3}. As N_h was of the order of 0.6–1 nm^{-3} this means that the volume which contains one hole, $1/N_\mathrm{h}$, is around 1–1.6 nm^3.

3.6. Free volume and structural dynamics

In the following section dielectric relaxation data are analysed according to a modified version of the Cohen–Turnbull free volume model [2]. Using statistical mechanical arguments these authors derived that the size distribution of the free

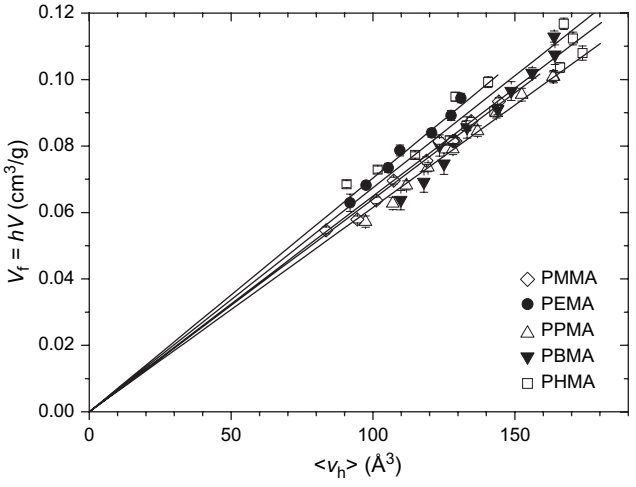

Fig. 10. Specific free volume $V_\mathrm{f}(T)$ plotted as a function of the mean hole volume, $\langle v_\mathrm{h}(T)\rangle$. Lines show linear fits constrained to pass through the origin.

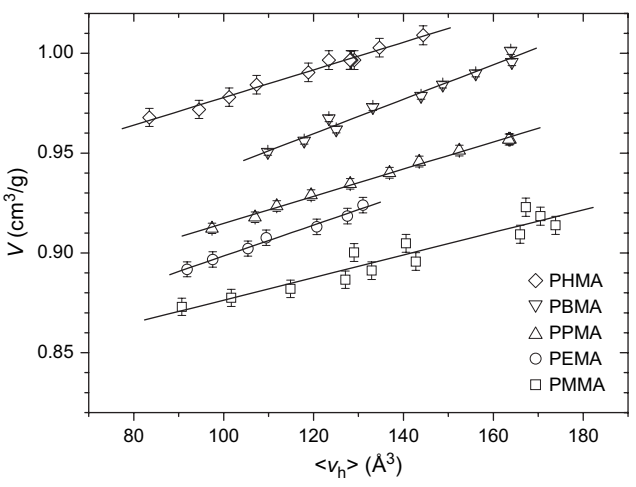

Fig. 11. Specific volume $V(T)$ plotted as a function of the mean hole volume, $\langle v_\mathrm{h}(T)\rangle$. Lines show linear fits.

volume per molecule follows an exponential decreasing function. When applying this approach to a structural relaxation process in a melt its frequency, ω, is given by:

$$\omega = C\exp\left(-\frac{\gamma V_f^*}{V_f}\right) \tag{8}$$

where γV_f^* is the minimum specific free volume required for the relaxation process and γ is introduced to account for the overlap of two or more molecules' free volume and is in the range 0.5–1. The relaxation angular frequencies used in this work come from reconstructions using the VFT equation $\log\omega = \log\Omega - (B/\ln 10)/(T - T_0)$ with the parameters for the α-relaxation ($\log\Omega_\alpha$, B_α and $T_{0\alpha}$ – see (our) Table 2, [48]) given by Beiner et al. for PMMA, PEMA, PBMA and also by fitting the values in Fig. 5 in Ref. [21] to generate VFT parameters for PPMA and PHMA. Plotting $\log\omega$ against $1/V_f$ should, according to Eq. (8), result in a straight line plot. It can be seen in Fig. 12 that this is not the case; there is a curvature in the plots. This curvature has been observed before and an alternative linearisation is achieved by substituting $1/V_f$ by $1/(V_f - \Delta V)$ (see ref. [13] and references therein). It has been pointed out that Eq. (8) can be considered as being equivalent to the VFT equation if one assumes a linear expansion of free volume, $V_f = E_f(T - T_0')$. In this case we should have $T_0 = T_0'$ and $B = \gamma V_f^*/E_f$. As we found, however, $T_0' < T_0$. Substituting $1/V_f$ by $1/(V_f - \Delta V)$ with $\Delta V = E_f(T_0 - T_0')$ is a way of incorporating this fact.

A method for determining ΔV via the relaxation plots was recently suggested by Dlubek et al. [45] who, adapting a method proposed by Stickel et al. [49], differentiated Eq. (8) with $1/V_f$ replaced by $1/(V_f - \Delta V)$ to get:

$$\left[\mathrm{d}\log\omega/\mathrm{d}V_f\right]^{-1/2} = \frac{\left[\mathrm{d}\log\omega/\mathrm{d}T\right]^{-1/2}}{\left[\mathrm{d}V_f/\mathrm{d}T\right]^{-1/2}} = \left(\frac{\gamma V_f^*}{\ln 10}\right)^{-1/2}\left(V_f - \Delta V\right) \tag{9}$$

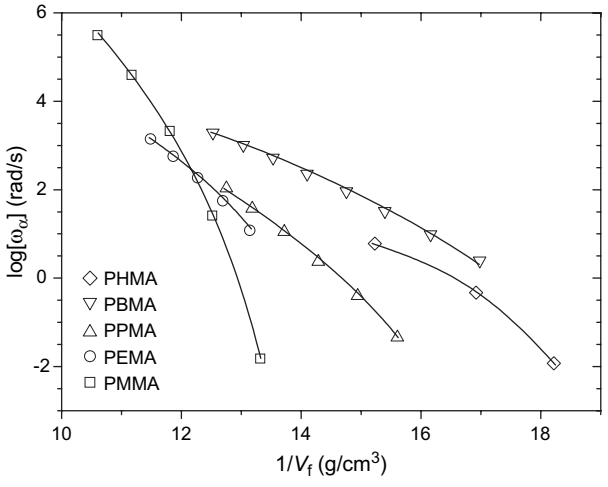

Fig. 12. "Modified" relaxation map (Cohen–Turnbull plot) of the characteristic (circular) frequency of the α-relaxation (maximum of the ε''-curve from dielectric relaxation experiments, taken from Beiner et al. [21,48]), $\log\omega_\alpha$, against $1/V_f$ where $V_f = N_h'\langle v_h\rangle$. Lines are to guide the eyes only. Points shown are above T_g.

Thus by plotting $[\mathrm{d}\log\omega/\mathrm{d}V_f]^{-1/2}$ against V_f (Fig. 13) and fitting straight lines to these data, values of γV_f^* and ΔV are obtained, which are listed in Table 2. It can be seen that ΔV decreases from $C = 1$ to $C = 4$, but then increases again to $C = 6$; no strong trend is observed for γV_f^*.

It has been suggested recently by some of the authors [13] that $\Delta V > 0$ is indicative of a fraction of the free volume as calculated by the S–S eos not being involved in the main relaxation process. It is reasonable to suggest that the free volume that is active in the relaxations, $V_f - \Delta V$, is present only in groups of empty S–S cells bigger than a certain cut-off, below which insufficient free volume is available for its free exchange due to standard thermal fluctuations. This is similar in concept to a two-phase model of solid-like and liquid-like clusters used in Cohen and Grest's free volume approach to the glass transition [50].

The idea of considering S–S cells in clusters was explored quantitatively by Vleeshouwers et al. [51] who performed Monte Carlo simulations to obtain the cluster size distribution of S–S cells as a function of the hole fraction, h. The MC results were represented empirically by a decreasing exponential-like function, describing the probability of a cell being in a cluster of i cells. For the materials in this study it is therefore possible, using the temperature dependence of h calculated above, to calculate the proportion of free volume existing in clusters of size i cells for each temperature. If p_i is the fraction of free volume present in agglomerates containing i vacant cells ($\Sigma p_i = 1$, $i = 1 - \infty$), then the partial free volume containing multivacancies of m or more cells is:

$$V_f^m = V_f\sum_{i=m}^{\infty} p_i \tag{10}$$

Fig. 14 shows V_f^m as a function of temperature for PMMA. As can be seen, above T_g the increase of V_f^m with temperature can be approximately described by a straight line, particularly for low m. As m increases, more curvature is seen in the plots as T_g is approached from above. The temperature where V_f^m

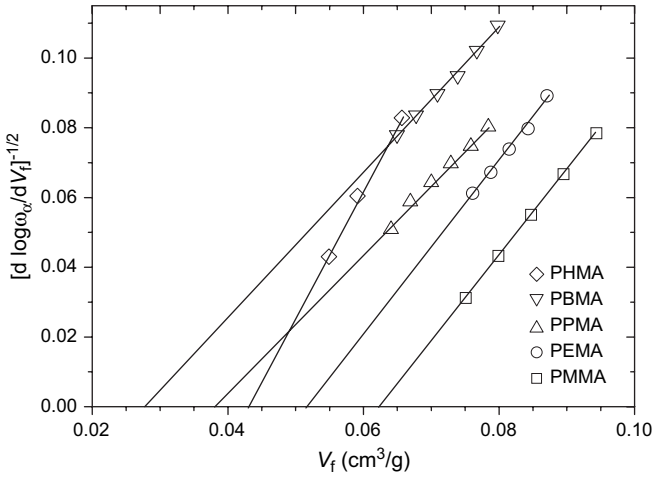

Fig. 13. Plot of $[\mathrm{d}\log\omega/\mathrm{d}V_f]^{-1/2}$ against $V_f = N_h'\langle v_h\rangle$ for the series of poly(alkyl methacylate)s. Lines are least-square fits to the data between T_g and T_+; $\log \equiv \log_{10}$.

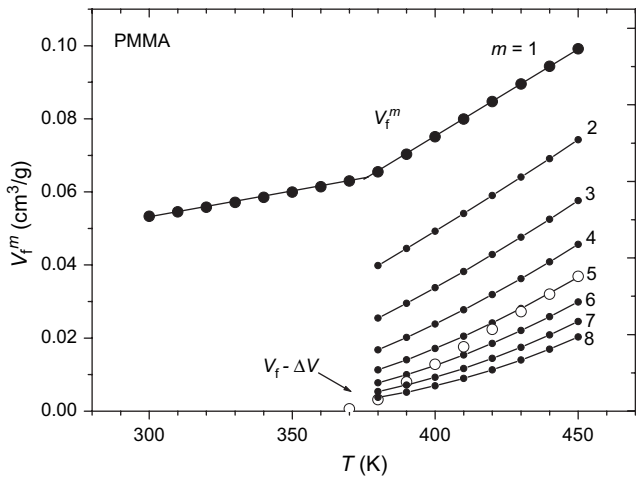

Fig. 14. Specific free volume V_f^m in aggregates containing m or more empty S–S cells for PMMA. The data for $m = 1$ (filled large circles) represent the total specific free volume whereas those for $m = 2, 3, 4, 5, 6$ (small dots connected by lines – data shown above T_g) represent decreasing fractions of the total free volume. Compared with this is the quantity $V_f - \Delta V$, calculated using $\Delta V = 0.060$. Values for ΔV for other materials are listed in Table 2.

becomes zero when linearly extrapolated from far above T_g increases with increasing m. Also shown in Fig. 14 is the variation of $V_f - \Delta V$ with ΔV as obtained from Fig. 13. From this it can be seen that the α-relaxation as measured by dielectric experiments follows the Cohen–Turnbull free volume theory as applied to aggregates of empty S–S cells with (on average) between ~8 (380 K) and ~5 (450 K) cells in them. A similar procedure was followed for the other materials and groups of ~3.8 (PEMA), ~2.7 (PPMA), ~2 (PBMA) and ~2.9 (PHMA) cells were found to be required for the relaxations. A collection of m cells corresponds to a volume of $m \times v_{SS}$ (v_{SS} values at T_g – though v_{SS} varies slowly with temperature and is, to a first approximation, constant – calculated above and are listed in Table 1), which for these materials are 399 Å^3 (380 K) or 250 Å^3 (450 K) (PMMA), 200 Å^3 (PEMA), 144 Å^3 (PPMA) and 105 Å^3 (PBMA), all ±15 Å^3. Recently some of the authors found for PVAc a minimum cluster size of 3 [13]. The decrease in the aggregate size shows that with increasing C-number smaller local free volumes are sufficient to exhibit a liquid-like behaviour in its surroundings. These results correlate well with the decrease in T_g.

4. Conclusions

Free volume data from positron annihilation lifetime spectroscopy (PALS) experiments are reported for a series of poly(n-alkyl methacrylate)s. T_gs are found to decrease from 382 to 224 ± 5 K as the side-chain length increases from methyl to hexyl. This is accompanied by a general increase in free volume hole size in the temperature ranges measured. The thermal expansivities of the mean hole volume increase below T_g, e_{hg}, from 0.13 to 0.28 ± 0.03 Å^3/K as the side-chain increases, and is constant above T_g, e_{hr}, around 1 Å^3/K. This is presented as evidence of an internal plasticization whereby the side-chains reduce effective packing of molecules. Pressure–volume–temperature (PVT) data are also presented and analysed using the Simha–Somcynsky (S–S) equation of state. From this, the specific occupied and free volumes for the full range of temperatures and pressures can be calculated. The specific free volume variations match those from PALS experiments. By comparing PALS and PVT data, the number hole density per mass unit, N_h', is calculated; using different methods this varies between 0.54 and 0.86 × 10^{21} g^{-1}.

An attempt is made to model-free volume contributions to molecular mobility in a series of poly(n-alkyl methacrylate)s using a modified version of the free volume theory of Cohen and Turnbull. We observed that with decreasing temperature the α-relaxation detected via dielectric measurements slows down faster than the shrinkage of hole free volume V_f would predict on the basis of the free volume theory. V_f becomes zero only significantly below the Vogel temperature T_0, $T_0 - T_0' = 46$–105 K. Plots of the α-relaxation frequency $\log \omega$ vs. $1/V_f$ can be linearised when taking into account this discrepancy by substituting $1/V_f$ by $1/(V_f - \Delta V)$ with $\Delta V = E_f(T_0 - T_0')$. ΔV varies between 0.062 and 0.027 ± 0.003 cm^3/g. One possible interpretation of this is that the α-relaxation only occurs when a group of m or more unoccupied S–S cells are aggregated together. m is found to vary between 8 and 2 for poly(methyl methacrylate) and poly(n-butyl methacrylate), respectively. This indicates the increasing flexibility of chains with increasing side-chain length caused by the increasing fraction of polyethylene-like chain parts. We found in the free volume expansion no specific feature in coincidence with the dynamic crossover.

Acknowledgements

We thank Dr. M. Beiner (Halle) for providing us with the samples and the dynamic data as well as for helpful comments to polymer dynamics. We are grateful to Mr. H. Knuth (Dresden) for technical assistance in PVT experiments.

References

[1] Doolittle A. J Appl Phys 1951;21(12):1471.
[2] Cohen M, Turnbull D. J Chem Phys 1959;31(5):1164.
[3] Mogensen OE. Positron annihilation in chemistry. Berlin: Springer; 1995.
[4] Pethrick R. Prog Polym Sci 1997;22:1.
[5] Eldrup M, Lightbody D, Sherwood JN. Chem Phys 1981;63:51.
[6] Hofmann D, Heuchel M, Yampolskii Y, Khotimskii V, Shanterovich V. Macromolecules 2002;35:2129.
[7] Bamford D, Reiche A, Dlubek G, Alloin F, Sanchez J-Y, Alam MA. J Chem Phys 2003;118(20):9420.
[8] Vogel H. Phys Z 1921;22:645.
[9] Fulcher GS. J Am Ceram Soc 1925;8:339.
[10] Tammann G, Hesse W. Z Anorg Allg Chem 1926;156:245.
[11] Bartoš J, Krištiak J, Šauša O, Zrubcová J. Macromol Symp 2000;158:111.
[12] Williams M, Landel R, Ferry J. J Am Chem Soc 1955;77:3701.
[13] Dlubek G, Kilburn D, Alam MA. Macromol Chem Phys 2005;206:818.
[14] Simha R, Somcynsky T. Macromolecules 1969;2(4):342.
[15] Simha R. Macromolecules 1977;10(5):1025.
[16] Hijmans J. Physica 1961;27:433.
[17] Schmidt M, Maurer FHJ. Macromolecules 2000;33:3879.
[18] Kilburn D, Bamford D, Dlubek G, Pionteck J, Alam MA. J Polym Sci Part B Polym Phys 2003;41:3089.

[19] Dlubek G, Stejny J, Alam MA. Macromolecules 1998;31:4574.
[20] Kahle S, Hempel E, Beiner M, Unger R, Schröter K, Donth E. J Mol Struct 1999;479:149.
[21] Beiner M. Macromol Rapid Commun 2001;22:869.
[22] Garwe F, Schönhals A, Lockwenz H, Beiner M, Schröter K, Donth E. Macromolecules 1996;29:247.
[23] Beiner M, Kahle S, Abens S, Hempel H, Höring S, Meissner M, et al. Macromolecules 2001;34:5927.
[24] Hempel E, Kahle S, Unger R, Donth E. Thermochim Acta 1999;329:97.
[25] Malhotra BD, Pethrick RA. Macromolecules 1983;16:1175.
[26] Li HL, Ujihira Y, Tanaka S, Yamahita T, Horie K. J Radioanal Nucl Chem 1996;210(2):543.
[27] Zoller P, Walsh CJ. Standard pressure–volume–temperature data for polymers. Lancaster, Basel: Technomic Publ Co, Inc; 1995.
[28] Rogers S, Mandelkern L. J Phys Chem 1957;61(7):985.
[29] Utracki L, Simha R. Macromol Theory Simul 2001;10:17.
[30] Wilson PS, Simha R. Macromolecules 1973;6(6):908.
[31] Simha R, Carri G. J Polym Sci Part B Polym Phys 1994;32:2645.
[32] Tao SJ. J Chem Phys 1972;56:5499.
[33] Kansy J. Nucl Instrum Methods Phys Res Sect A 1996;374:235.
[34] Kansy J. LT for Windows, Version 9.0. Inst of Phys Chem of Metals, Silesian University, Bankowa 12, PL-40-007 Katowice, Poland; March 2002. Private communication.
[35] Baugher AH, Kossler WJ, Petzinger KG. Macromolecules 1996;29:7280.
[36] Dlubek G, De U, Pionteck J, Arutyunov NYu, Edelmann M, Krause-Rehberg R. Macromol Chem Phys 2005;206:827.
[37] Dlubek G, Sen Gupta A, Pionteck J, Krause-Rehberg R, Kaspar H, Lochhaas K. Macromolecules 2004;37:6606.
[38] Schmidt M, Maurer FHJ. Polymer 2000;41:8419.
[39] Wang CL, Hirade T, Maurer FHJ, Eldrup M, Pedersen J. J Chem Phys 1998;108(11):4654.
[40] Kilburn D, Dlubek G, Pionteck J, Bamford D, Alam MA. Polymer 2005; 46:869.
[41] Dlubek G, Bamford D, Rodriguez-Gonzalez A, Bornemann S, Stejny J, Schade B, et al. J Polym Sci B Polym Phys 2002;40:434.
[42] Beiner M, Schröter K, Hempel E, Reissig S, Donth E. Macromolecules 1999;32:6278.
[43] Donth EJ. The glass transition: relaxation dynamics in liquids and disordered materials. Berlin: Springer; 2001.
[44] Ngai KL, Li-R Bao, Yee AF, Soles CL. Phys Rev Lett 2001;87(21): 215901.
[45] Dlubek G, Hassan EM, Krause-Rehberg R, Pionteck J. Phys Rev E 2006; 73:031803.
[46] Bartoš J, Šauša O, Krištiak J, Blochowicz T, Rössler E. J Phys Condens Mater 2001;13:11473.
[47] Bartoš J, Šauša O, Bandzuch P, Zrubcová J, Krištiak J. J Non-Cryst Solids 2002;307–310:417.
[48] Beiner M, Huth H, Schröter K. J Non-Cryst Solids 2001;279:126.
[49] Stickel F, Fischer W, Richert R. J Chem Phys 1995;102(15):6251.
[50] Cohen MH, Grest GS. Phys Rev B 1979;20(3):1077.
[51] Vleeshouwers S, Kluin JE, McGervey JD, Jamieson AM, Simha R. J Polym Sci B Polym Phys 1992;30:142.